Interaction with Membrane Lipids and Heme Ligand Binding Properties of *Escherichia coli* Flavohemoglobin†

Alessandra Bonamore,‡ Anna Farina,‡ Maurizio Gattoni, M. Eugenia Schininà, Andrea Bellelli, and Alberto Boffi*

CNR Istituto di Biologia e Patologia Molecolari and Department of Biochemical Sciences, University "La Sapienza" 00185 Rome, Italy

Received October 22, 2002; Revised Manuscript Received March 6, 2003

ABSTRACT: *Escherichia coli* flavohemoglobin has been shown to be able to bind specifically unsaturated and/or cyclopropanated fatty acids with very high affinity. Unsaturated or cyclopropanated fatty acid binding results in a modification of the visible absorption spectrum of the ferric heme, corresponding to a transition from a pentacoordinated (typical of the ligand free protein) to a hexacoordinated, high spin, heme iron. In contrast, no detectable interaction has been observed with saturated fatty acid, saturated phospholipids, linear, cyclic, and aromatic hydrocarbons pointing out that the protein recognizes specifically double bonds in cis conformation within the hydrocarbon chain of the fatty acid molecule. Accordingly, as demonstrated in gel filtration experiments, flavohemoglobin is able to bind liposomes obtained from lipid extracts of *E. coli* membranes and eventually abstract phospholipids containing cis double bonds and/or cyclopropane rings along the acyl chains. The presence of a protein bound lipid strongly affects the thermodynamic and kinetic properties of imidazole binding to the ferric protein and brings about significant modifications in the reactivity of the ferrous protein with oxygen and carbon monoxide. The effect of the bound lipid has been accounted for by a reaction scheme that involves the presence of two sites for the lipid/ligand recognition, namely, the heme iron and a non-heme site located in a loop region above the heme pocket.

Escherichia coli flavohemoglobin (HMP) is an oxygen binding protein composed of a globin domain fused with a ferredoxin reductase-like FAD- and NAD-binding module. HMP belongs to the increasingly growing family of hemoglobin-like proteins whose genes have been identified in a wide variety of prokaryotic and eukaryotic microorganisms and whose functional annotations are still doubtful (*1*). A possible physiological function for HMP has been proposed in the framework of the response of the bacterial cell to nitrosative stress on the basis of the observation that protein expression is enhanced in the presence of nitric oxide releasers in the culture medium (*2*). Accordingly, HMP is able to catalize the oxidation of free NO to nitrate both in vivo and in vitro in the presence of oxygen and NADH (*3*−*6*). More recently, the NO dioxygenase activity has been challenged in favor of an NO denitrosylase function in which, at low (physiologically relevant) oxygen tensions, HMP turns over in the ferric state with the intermediacy of an iron bound nitroxyl anion that is subsequently transformed into nitrate in the presence of oxygen (*7*).

Nevertheless, although the major functional hypotheses for HMP are centered around NO scavenging, a number of experimental observations carried out on highly similar proteins have revealed different possible scenarios for bacterial hemoglobins' functions. In particular, the presence of a tightly bound phospholipid within the heme pocket of *Alcaligenes Eutrophus* flavohemoglobin initially suggested the participation of bacterial hemoglobins to some sort of lipid membrane transport and/or processing (*8*). More recently, the single chain bacterial hemoglobin from *Vitreoscilla* sp. (VHB) and the truncated hemoglobin from *Mycobacterium tubercolosis* (HbO) have been reported to be preferentially localized in contact with the bacterial inner membrane in vivo and to be capable of reversible binding to liposomes obtained from bacterial lipid extracts in vitro (*9*, *10*). HMP itself has also been reported to interact with membrane phospholipids although with no apparent specificity for any kind of lipid molecule (*8*). Along the same line, the three-dimensional structures of the ferrous, lipid bound, flavohemoglobin from *A. eutrophus* (FHP) (*11*), of the ferric (ligand free) *Vitreoscilla* Hb (*12*), and the ferric ligand free HMP (*13*) not only revealed a high degree of structural similarity in the three proteins but also pointed out that lipid binding contact regions are conserved (*13*). All together, these data prompted the present investigation on the lipid binding properties of HMP and on the effect of the bound lipids on the thermodynamic and kinetics of ligand binding to the heme iron.

EXPERIMENTAL PROCEDURES

HMP has been expressed and purified as reported previously (*14*). Protein concentration was measured spectrophotometrically using the extinction coefficient of 156 000 M^{-1} cm^{-1} at 421 nm for the ferric cyanide adduct.

† This work was supported by grants from Ministero Istruzione Università Ricerca for the "Centro di Eccellenza Biologia e Medicina Molecolare" and 40% (to A.B.).

* Corresponding author. Fax: 39 06 4440062. E-mail: alberto.boffi@uniroma1.it.

‡ These authors contributed equally to this work.

10.1021/bi0206311 CCC: $25.00
Published on Web 04/26/2003

Lipid Binding Properties of Ferric HMP. Purified, lipid free protein has been screened for heme visible absorption spectral changes against a number of phospholipids (dipalmitoil phosphatidil choline, dipalmitoil phosphatidil ethanolamine, dipalmitoil phosphatidic acid), saturated (palmitic and stearic), unsaturated (oleic, palmitoleic, linoleic, cis vaccenic), and cyclopropanated (9,10-methylen palmitoleic) fatty acids and their methyl esters, aromatic hydrocarbons (benzene, toluene, naftalene), and linear and cyclic alkenes (1-dodecene, 6-dodecene, cyclohexene, cyclooctene). The screening was performed on 8−12 μM protein solutions in 0.1 M phosphate buffer at pH 7.0 and 20 °C containing 20% v/v ethanol by adding increasing amounts of ligand (1−100 molar excess) dissolved in ethanol. All reagents were from Sigma Aldrich Co. with the exception of cyclopropan palmitoleic acid (Larodan Fine Chemicals, Malmö, Sweden). Fatty acid binding kinetics were performed by mixing 5 μM HMP in 0.1 M phosphate buffer at pH 7.0 and 20 °C containing 20% v/v ethanol with a solution containing increasing amounts of palmitoleic, cyclopropanpalmitoleic, or linoleic acid dissolved in the same buffer in an Applied Photophysics stopped flow apparatus (Leatherhead, UK). Fatty acid release kinetics were estimated in competition essays with the lipid avid hydroxylalkoxypropyl-dextrane resin (Tipe X, Sigma Aldrich Co.). A total of 5 mL of a gel suspension containing 20 mg of dried resin in 0.1 M phosphate buffer at pH 7.0 and 20% v/v ethanol were placed in a small beaker under stirring at 20 °C. The fiber optic Dip Probe of a Varian Cary 50 spectrophopometer, equipped with a 150 W pulsed Xe lamp (Varian Instrument Co. Australia), was immersed in the suspension, and a baseline was recorded. A HMP solution (100 μL, 160 μM) saturated with oleic, cyclopropan-palmitoleic, or linoleic acid was then added to the suspension, and spectra were measured in sequential mode (9 s for each spectrum). Fatty acid release was monitored by following the spectral changes in the Soret region.

Total *E. coli* lipid extracts (TLE) were prepared according to Bligh and Dyer (*15*). Briefly, 250 mg of *Escherichia coli* pellets obtained after sonication and centrifugation of whole cells were washed with the lysis buffer, dried under vacuum at −5 °C, and dissolved in 5 mL of a methanol/chloroform (2:1 v/v) solution. The solution was vortexed at room temperature and stored at 4 °C for 24 h. Thereafter, the sample was centrifuged at 6000 rpm, the supernatant was kept at 4 °C, and the pellet was subjected to a new extraction procedure as before. Then, 5 mL of chloroform and 5 mL of water were added to the chloroform methanol supernatants, and the chloroform phase was separated, dried under nitrogen gas at 4 °C, and stored at −20 °C. The effective removal of protein components from the lipid extracts was checked by IR spectroscopy (absence of the 1650 cm^{-1} amide band).

Gel filtration experiments were carried out according to Chiancone et al. (*16*). A Sephadex G-75 (Pharmacia, Uppsala, Sweden) column (0.5 × 35 cm) was used at a constant flow rate of 5 mL/h and at 20 °C. All experiments were carried out in 50 mM phosphate buffer at pH 7.0. A total of 0.2 mL of a protein solution (25 μM) were applied on the column, and the elution profiles was monitored in the Soret region with a Jasco 7800 spectrophotometer equipped with a thermostated flow cell. Column calibration was determined by using native human hemoglobin tetramer (carbonmonoxy derivative) and horse heart myoglobin. Liposomes were obtained from dried TLE resuspended in 10 mL of 50 mM phosphate buffer at pH 7.0, heated at 60 °C for 15 min, and then sonicated in a Soniprep 150 sonicator for 30 min. The liposomes thus obtained were left 4 h at 4 °C, pelleted by centrifugation, and resuspended in buffer before use. Phospholipid content in TLE was determined by FTIR absorption of the carboxyl ester at 1735 cm^{-1} on a weighted amount of dry TLE dissolved in chloroform with respect to a phosphatidylethanolamine standard (Sigma Aldrich Co.). Liposome solutions (0.4 mL) containing 20:1 phospholipid/protein molar excess were mixed with 0.1 mL of HMP solutions (25 μM) and then applied on the G-75 column. Horse Mb (Sigma Aldrich Co.) was also run in gel filtration experiments in the presence of TLE as a control.

For mass spectrometry measurements, the fatty acids were extracted as follows: the reaction mixure containing 20 μM HMP in 0.1 M pH 7.0, 40 μM UFA and/or CFA, 250 μM NADH, and 270 μM O_2 was allowed to stand until full oxidation of NADH and then mixed with a chloroform/methanol (4:1 v/v) solution, vortexed, and centrifuged at 6000 rpm for 15 min. The chloroform/methanol extracts were dried under vacum and resuspended in 80% methanol/water containing 0.5% v/v ammonia. The fatty acid containing methanolic solutions were analyzed by infusion (5 mL/nvv) in an electrospray ion trap mass spectrometer (ES-IT, mod. LCQ, ThermoFinnigan, San Jose, CA). Authentic fatty acid standards, dissolved in the same solvent, were used to optimize the ESI source parameters as follows: sheath gas (nitrogen) flow rate, 90 (arbitrary unit); electrospray needle voltage, 40 kV; capillary voltage and temperature, −12 V and 180 °C, respectively; and electron multiplier and conversion dynode, −800 V and −15 kV, respectively. The mass spectra were collected over the mass range of 50−500 amu, in negative ion mode.

Heme−Iron Ligand Binding Properties of Ferric HMP. Imidazole titration experiments were carried out on both lipid free and lipid (UFA, CFA, or TLE) saturated ferric protein by adding small volumes of ligand solutions to the protein solution (8 μM) in 0.1 M phosphate buffer at pH 7.0 and 20 °C in a 1 cm quartz cuvette. Absorption spectra were recorded after each ligand addition (2 min equilibration time) on a Jasco V-570 spectrophotometer (Jasco Ltd., Japan). The titration profiles of lipid bound HMP were fitted to the simple, one binding site, reaction (Figure 1, Scheme 1). Imidazole equilibrium binding curves of lipid free HMP were fitted to the reaction Scheme 2 (Figure 1). The presence of two ligand binding sites in Scheme 2 may appear paradoxical in a monomeric hemeoprotein. Nevertheless, the presence of a single difference spectrum upon ligand binding (see below) together with the strongly biphasic titration profile suggests an unusual mechanism of ligand saturation. The binding polynomial obtained from Scheme 2 is (see also legend of Figure 1)

$$Y = \frac{[\mathrm{x{-}P{\sim}}] + [\mathrm{{-}P{\sim}x}] + 2[\mathrm{x{-}P^{*}{\sim}x}]}{2C_{\mathrm{tot}}} = \frac{K_1x + K_2x + 2K_4K_1x^2}{2\{1 + K_1x + K_2x + K_4K_1x^2\}} \quad (1)$$

where x−P∼ represents the protein with heme bound

Scheme I

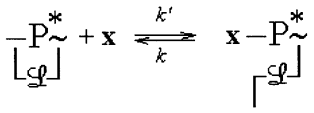

Scheme II

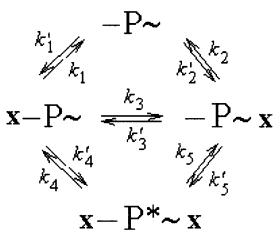

FIGURE 1: Reaction schemes for ligand binding to ferric *E. coli* flavohemoglobin. Ferric HMP has been inferred to possess a heme iron ligand binding site (-P) and a non heme binding site (P∼). Both sites are involved in the recognition of lipid (UFA or CFA) substrates ( ). The interaction of the lipid with the heme site is weak and can be diplaced by heme iron ligands (x), as depicted in Scheme 1. Complete removal of the bound lipid renders the non-heme site available for ligand interaction as outlined in Scheme 2. The ligand binds to the heme iron and is accompanied by a fast ligand exchange (k_3 and k_{-3}) between the heme and the non-heme binding sites. Full saturation of both sites implies a conformational transition from P to P* species.

imidazole, −P∼x is the protein with imidazole bound in the non-heme site, and x−P*∼x is the doubly ligated species in which both the heme and the non-heme site are occupied by the imidazole ligand. It is important to point out that the biphasic imidazole titration profiles cannot be corrected for the contribution of species spectrally different from that of unliganded and fully liganded derivatives. In other words, all spectra obtained within the imidazole titration experiments are accounted for a linear combination of the unliganded derivative and of the fully ligated adduct (see also ref *13*). The observed biphasic titration profiles can be fully described in terms of Scheme 2 of Figure 1 under the assumption that imidazole binding to the non-heme site is spectroscopically silent. Hence, the species −P∼x does not contribute to the observed signal, the species x−P*∼x yields the same spectral contribution as x−P∼, and the observed signal was fitted to a modified binding polynomial

$$Y_{obs} = \frac{[x-P\sim] + [x-P^*\sim x]}{C_{tot}} = \frac{K_1 x + K_4 K_1 x^2}{1 + K_1 x + K_2 x + K_4 K_1 x^2} \quad (2)$$

Ligand combination kinetics were carried out by mixing the lipid free or TLE saturated protein solutions (6−8 μM) with imidazole solutions in an applied photophysics rapid mixing apparatus (Applied Photophysics, Leatherhead, UK).

To single out the rate constants of Scheme 2 (Figure 1), the following procedure was adopted: (i) only the spectral transitions involving imidazole binding or release to the heme site are considered to contribute to the observed signal; (ii) the set of imidazole combination time courses were fitted to Scheme 2 (Figure 1) by fixing the equilibrium thermodynamic constants to the values obtained in the imidazole titration experiment. In this fitting procedure, it was assumed that the intramolecular process determined by K_3 is much faster with respect to the other processes. Hence, four rate constants, namely, k_1, k_2, k_4, and k_5 were allowed to float. The total Δ absorbances were fixed, for each time course, to the equilibrium values. The Matlab 5.0 program (The Math Works Inc. South Natick, MA) was used in all least-squares fitting procedures.

Heme−Iron Ligand Binding to Ferrous HMP. Oxygen release kinetics were carried out according to the oxygen pulse method (*17*). Briefly, the protein solutions containing 10−50 mM sodium dithionite were mixed with oxygen containing buffer. Oxygen binding to the heme iron occurs within the dead time of the instrument (4 ms) and is subsequently released due to the rapid reaction of oxygen itself with dithionite to produce higher sulfur oxides. Thus, the observed spectral signal pertains to the formation of deoxy heme and is monitored at the relevant Soret peak around 434 or at 415 nm (the peak of the oxygenated species). Slower absorbance changes (a decrease at 434 nm and an increase at 420 nm) were observed over tens of minutes time scale and were attributed to the binding of some dithionite byproducts to the heme iron and the subsequent formation of a hemochrome-like species. Such effects are dithionite concentration dependent and are negligible up to 50 mM dithionite. It was also observed that aged protein solutions (frozen at −70 °C for three months) exhibited almost complete hemochrome formation within a few minutes from dithionite addition. On the basis of these observations, oxygen pulse experiments were carried out on freshly prepared protein and were shown to be fully reproducible in different preparations up to 50−100 mM dithionite. The CO binding kinetics of HMP were measured in oxygen free solutions at pH 7.0 (0.1 M phosphate buffer), in the presence of 1 mM EDTA and 250 μM NADH, and 20.0 °C by laser photolysis. The HMP solution containing NADH was accurately degassed in a tonometer until the fully deoxy species was formed. Thereafter, the solution was equilibrated with CO gas at 20 °C to a final equilibrium concentration of 1−0.025 mM. The measurements have been carried out using as an optical pump the second harmonic from a Quanta System Nd:YAG laser (λ = 532 nm, frequency of 2 Hz with a pulse width of 5 ns and a pulse energy of approximately 80 mJ). The laser pulse flashes the sample in a tonometer with a fluorescence quartz cell of 1 cm length orthogonally to the optical probe due to a 100 W UV−vis source focused onto a monochromator SPEX 1681. Single wavelength measurements have been acquired using as a detector a photomultiplier tube Hamamatsu H6870. The time courses (average of 64 traces) were recorded using a digital oscilloscope Tektronix TDS 360. The time courses were followed at 434 nm, as a function of CO concentration (ranging between 1 and 0.025 mM) at a protein concentration of 4 μM.

RESULTS

Lipid Binding Properties of Ferric HMP. The present investigation originated from the observation of spectral changes in ferric HMP noticed during the protein purification procedure and initially attributed to the loss of flavin from the holoprotein. In particular, the visible absorption spectra of HMP before and after hydroxylapatite chromatography were different. Electrospray mass spectrometry, performed on the protein before hydroxylapatite chromatography, revealed the presence of heterogeneous protein-linked components attributed to phosphatidyl ethanol amine and phosphatidic acid derivatives, in full agreement with the report

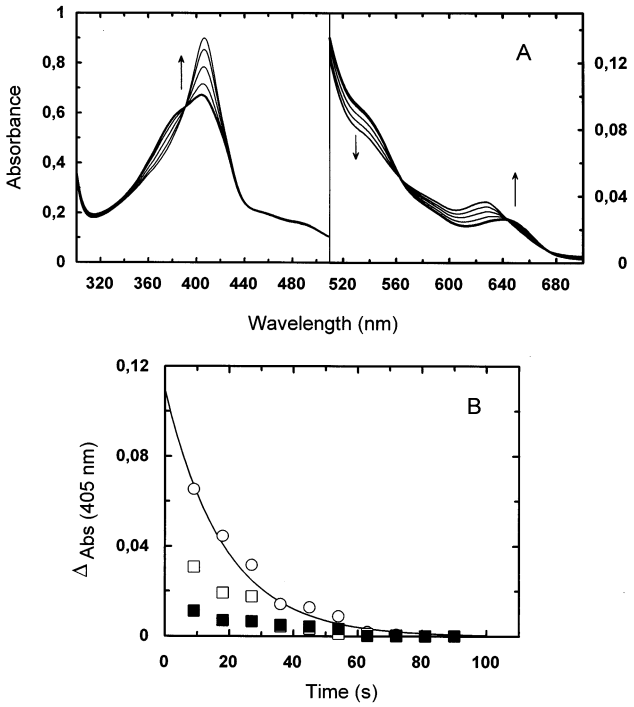

FIGURE 2: Spectral changes in the UV−vis absorption region accompanying lipid binding to ferric *E. coli* flavohemoglobin and kinetics of lipid release. A stoichiometric titration of lipid free, ferric HMP (12 μM heme) with an ethanol solution of oleic acid (3 μM per each addition) is shown in panel A. Panel B reports the kinetics of linoleic (○), oleic (■), and cyclopropan-palmitoleic (□) acid release from HMP as obtained in competition essays with hydroxyalkoxypropyl-dextrane. The continuous line represents the monoexponential fit to the linoleic acid data obtained by imposing the total absorbance change (at $t = 0$) to the calculated value ($k = 5 \pm 2.2 \times 10^{-2}$ s^{-1}). All experiments were carried out in 50 mM phosphate buffer at pH 7.0 in the presence of 20% v/v ethanol at 20 °C.

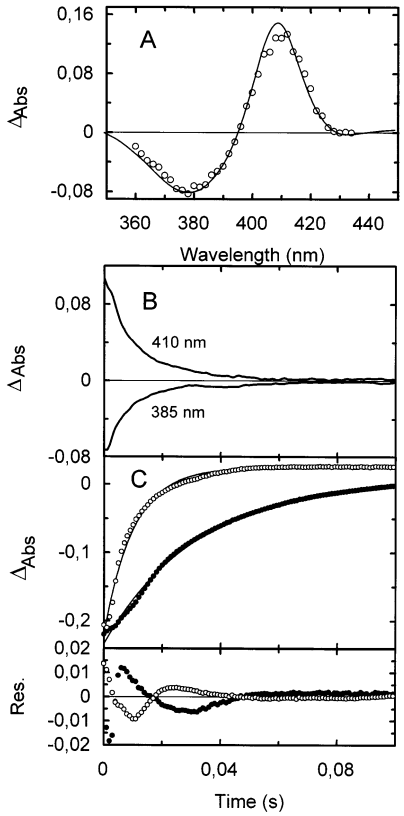

FIGURE 3: Kinetics of linoleic acid combination to ferric *E. coli* flavohemoglobin. Panel A shows the static (continuous line) and kinetic (○) difference spectra in the Soret region of linoleic acid bound ferric HMP minus lipid free ferric HMP. Time courses, as obtained in rapid mixing experiments at two selected wavelengths, are shown in panel B. The kinetics records obtained at all wavelengths were collected into a data matrix and averaged by standard procedures (see Experimental Procedures). The averaged traces are shown in panel C together with single-exponential fitting curves (continuous lines) and residuals. Apparent pseudo-first-order rates were 105 and 31 s^{-1}, respectively. Experimental conditions were protein concentration (after mixing), 5 μM; linoleic acid concentrations (after mixing), 5 × 10^{-5} M (○) and 2.5 × 10^{-5} M (●); and 0.1 M phosphate buffer, pH 7.0 containing 20% ethanol at 20 °C.

by Ollesch et al. (*8*). The removal of the phospholipid after hydroxylapatite chromatography was then directly correlated to the observed spectral changes. Full reversibility of the observed spectral transition was achieved by mixing the purified protein not only with total bacterial lipid extracts (TLE) but also with simple UFA and CFA free acids (see Figure 2). In contrast, no spectral changes have been detected by mixing HMP with ethanol solutions of methyl ester derivatives of UFA and CFA, saturated phospholipds, saturated fatty acids, linear, cyclic, and aromatic hydrocarbons. Subsequent titrations, carried out in buffers containing 20% v/v ethanol, pointed out that UFA and CFA bind to HMP with an extremely high affinity, even when the protein is pretreated with saturated fatty acids and/or saturated phospholipids. To strengthen the correlation between fatty acids binding and observed spectral signal and to estimate a value for the apparent affinity constant, a set of ligand combination kinetics were carried out by rapid mixing experiments. In these measurements, ferric HMP (in 20% ethanol) was mixed with increasing concentrations of palmitoleic, cyclopropanpalmitoleic, and linoleic acid under pseudo-first-order conditions. The time courses of linoleic acid binding to HMP as a function of wavelength and lipid concentration are reported in Figure 3. The time courses were collected into a data matrix and processed by a singular value decomposition (SVD) analysis to single out possible spectral intermediates. However, the procedure did not allow for an unequivocal deconvolution of the data set and eventually served to remove noise from the observed time courses. Fitting the (SVD) averaged time courses to single exponentials resulted in slightly biased time courses thus indicating that a more complex process than simple second-order binding underlines the lipid binding process to HMP. Fatty acid concentrations higher than 0.1 mM could not be obtained due to solubility problems; thus, a full pseudo-first-order plot could not be produced. The apparent second-order rate constant obtained from the fitting of the data of Figure 3C is around 2 × 10^6 M^{-1} s^{-1} (see also legend of Figure 3). Palmitoleic and cyclopropanpalmitoleic acids displayed time courses 6−7-fold faster than linoleic acid, and their kinetic parameters could not be estimated with certainty. A rough estimate of the lipid release rate was obtained by competition essays of lipid bound HMP with hydroxyalkoxypropyl dextrane. The results obtained, shown in Figure 2B, indicate that palmitoleic and cyclopropanpalmitoleic acids are rapidly released from HMP ($k > 0.1$ s^{-1}, assuming first-order release). In contrast, linoleic acid dissociates with an apparent rate of 5 × 10^{-2} s^{-1} thereby fixing the apparent affinity constant to a value of about 4 × 10^7 M^{-1} (in the presence of 20% ethanol).

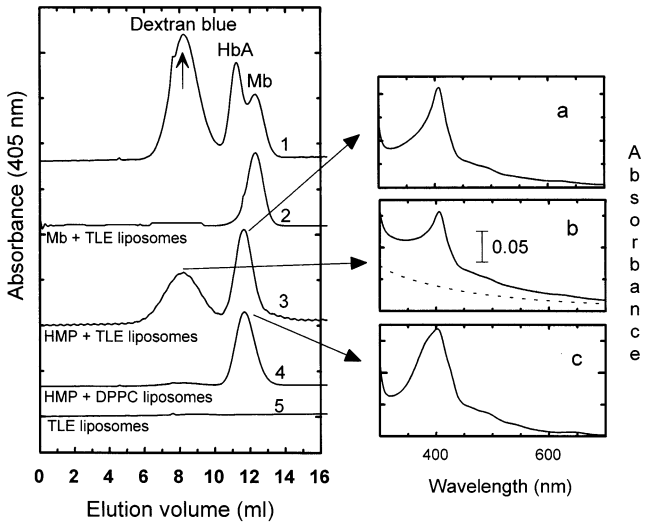

FIGURE 4: Elution profiles of *E. coli* flavohemoglobin on a gel filtration column in the presence of liposomes. From top to bottom: standard solution composed of of blue dextran (the arrows correspond to the excluded volume), carbonmonoxy human hemoglobin (HbA), and horse heart myoglobin (Mb) (profile 1); ferric Mb mixed with total lipid extracts (TLE) from *E. coli* cells (profile 2); purified ferric unliganded HMP mixed with liposomes (20:1 phospholipid/protein molar ratio) obtained from *E. coli* total lipid extracts (profile 3); purified ferric unliganded HMP mixed with DPPC liposomes (20:1 phospholipid protein molar ratio) (profile 4); and TLE liposomes (profile 5). The absorption spectra of the eluates relative to profiles 3 and 4 are also shown in panels a, b, and c, respectively. Experiments were carried out on a G-75 Sephadex column equilibrated with 50 mM phosphate buffer at pH 7.0 and 20 °C.

HMP binding to different types of liposomes was tested by means of gel filtration chromatography. The elution profiles reported in Figure 4 were obtained by measuring the absorption of the G-75 column eluate at the HMP Soret peak (405 nm for the ferric derivative and 420 nm for the CO bound ferrous derivative). The peak at 8.22 mL corresponds to the void volume as measured by dextran blue (Figure 4, profile 1). Liposomes are also eluted within the void volume as demonstrated by the slight absorbance increase around 8.3 mL (Figure 4, profile 5). Experiments carried out with freshly prepared TLE liposomes and horse Mb (ferric) indicated that the protein does not interact with the membranes and that no heme is released to the lipid bilayer under the present experimental conditions (Figure 4, profile 2). In apparent contrast, Ramandeep et al. (*9*) reported a weak but detectable interaction of both horse Mb and human hemoglobin with bacterial membranes. However, their size-exclusion measurements were at equilibrium (i.e., there was no mobile solvent phase through the gel matrix), whereas the present classical gel filtration experiment implies that even interacting particules (i.e., liposomes and Mb) can be sieved depending on their molecular mass if their interaction is weak. Thus, the present experiments cannot exclude a weak interaction between Mb and lipid bilayers. Moreover, heme release from ferric Mb to liposomes has been shown to be negligible at pH 7.0 and 20 °C whereas it does occur at pH values below 5.0 and temperature higher than 25 °C (unpublished data). In turn, the elution profile of HMP in the presence of TLE liposomes (Figure 4, profile 3) displays two separate peaks at 8.3 and 11.7 mL, respectively, whose integrated surfaces account for 55 and 45% of the total area. The peak at 8.3 mL contains both the TLE liposome fraction and the ferric HMP, whereas the peak at 11.7 corresponds to the elution volume of free HMP. The absorption spectra of the two fractions, shown in panels a and b of Figure 3, correspond to the spectrum of ferric, lipid bound, HMP. These data indicate clearly that HMP is not only capable of strong binding to liposomes obtained from *E. coli* lipid extracts (TLE) but may also abstract phospholipids from the liposome fraction, although it cannot be excluded that free, monodisperse lipids might be present in the liposome preparation even after centrifugation (see Experimental Procedures). Mass spectrometric analysis performed on the second fraction revealed the presence of a heterogeneous phospholipid species. The nature of the bound phospholipid, however, cannot be assessed with certainty due to the intrinsinc heterogeneity of the *sn*-1 and *sn*-2 glycerol linked components. As a control, purified, lipid free HMP was also screened toward dipalmitoil phosphatidil choline vescicles, and only a negligible interaction has been detected (Figure 4, profile 4).

Heme−Iron Ligand Binding Properties of Ferric HMP. Titration experiments of ferric HMP with imidazole yielded different results when performed with lipid free or UFA, CFA, or TLE saturated protein. In the present investigation, only the imidazole binding properties have been studied in detail since this ligand displays binding and release kinetics (see below) that are fast enaugh to allow for accurate equilibrium titrations even at very low ($<10^{-5}$ M) ligand concentrations. As shown in Figure 5, a simple single site titration profile is observed in the case of UFA (or CFA and TLE) saturated protein, whereas lipid free protein displays a strongly biphasic behavior characterized by a high affinity site ($C^1/_2$ around 1×10^{-5} M) and a low affinity one ($C^1/_2$ around 1×10^{-3} M). The overall affinity of lipid saturated protein for imidazole is drastically decreased with respect to the high affinity site in the lipid free protein and is centered around 3×10^3 M^{-1}. Fitting the equilibrium data with the binding polynomial given in eq 2 yielded a complete set of thermodynamic constants whose values are reported in Table 2. Such a minimal reaction scheme imposes severe contraints on the values of the equilibrium constants. In particular, the value of K_3 appears to be frozen around unity as it determines the amplitudes of the two phases and thus the flexus in the titration profile. As a consequence, $K_1 \approx K_2$ and $K_4 \approx K_5$ thus implying that the intrinsic affinity of the ligand molecule for the heme site and for the non-heme site is very similar. Such a stiff condition, however, was fulfilled by the analysis of the reaction kinetics reported below and can be physically allowed by the considerations given in the Discussion. In Figure 5, control experiments performed on horse Mb are also shown. These data indicate that the imidazole titration profile of the protein is unaffected by the presence of TLE (10 molar excess of lipids with respect to the protein).

The kinetic behavior of imidazole binding to HMP has been thoroughly analyzed in rapid mixing experiments. Imidazole binding kinetics of lipid bound (TLE) HMP is accounted for a simple second-order process with a rate constant of 8×10^4 M^{-1} s^{-1} (see Figure 6B). The rate of imidazole release calculated from the ratio between the second-order rate and the equilibrium constants (3.6×10^3 M^{-1}) is 22 s^{-1}, whereas the same constant obtained from the pseudo-first-order plot (intercept with the *Y* axis) is

Table 1: Phospholipids and Fatty Acids Binding to *E. coli* Flavohemoglobin as Screened by UV−vis Spectroscopy and ESI Mass Spectrometry

lipid type	UV−vis spectral changes	ESI mass MW (g mol^{-1})
L-α dipalmitoyl phosphatidyl choline	−	
L-α dipalmitoyl phosphatidyl ethanolamine	−	
L-α dipalmitoyl phosphatidyc acid	−	
palmitic acid	−	
stearic acid	−	
oleic acid	+	282 (282.5)[a]
palmitoleic acid	+	254 (254.4)
linoleic acid	+	278 (278.2)
cis vaccenic acid	+	282 (282.5)
9,10-methylen palmitoleic	+	265 (265.2)
aromatic hydrocarbons (benzene, toluene, naftalene)	−	
linear and cyclic alkenes (1 dodecene, 6 dodecene, cyclohexene, cyclooctene)	−	

[a] Number in parentheses indicate the calculated monoisotopic molecular weight.

Table 2: Summary of Thermodynamic and Kinetic Parameters for Imidazole Binding to Ferric, Lipid Free, *E. coli* Flavohemoglobin

	equilibrium constants[a]	rate constants[b]	(s^{-1})
K_1	$2.0 \pm 0.15 \times 10^5$ M^{-1}	k_1	22
K_2	$2.2 \pm 0.25 \times 10^5$ M^{-1}	k_2	0.3
K_3	1.1	k_3	>1000
K_4	$6.6 \pm 0.3 \times 10^3$ M^{-1}	k_4	0.05
K_5	6.0×10^3 M^{-1}	k_5	4

[a] The equilibrium constants for imidazole binding to HMP were obtained by fitting the data of Figure 4 to the binding polynomial relative to the reaction Scheme 2 (Figure 1) (eq 2). The rate constants were obtained according to the global fitting procedure of the data shown in Figure 6A to the reaction Scheme 2 (Figure 1) (see Experimental Procedures). [b] In the data fitting of the rate constants, the equilibrium constants K_1 to K_5 were fixed, and the first-order rates of ligand release were allowed to float. Thus, the combination rate constants (k_1', k_2', k_4', and k_5') can be obtained from the equilibrium constants and the dissociation rate constants. The values of the ligand release constants are devoid of standard deviations as they are the result of a global fitting procedure (see Experimental Procedures and Results sections for details). K_3 and K_5 values are automatically determined according to Scheme 2, Figure 1.

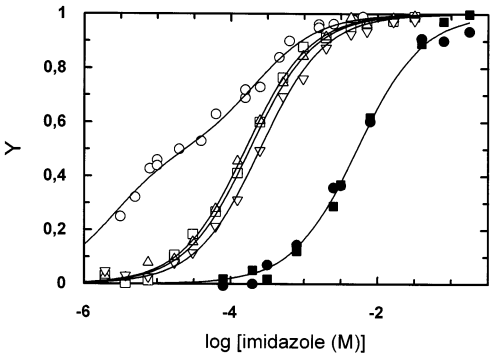

FIGURE 5: Ligand binding isotherms of ferric *E. coli* flavohemoglobin and horse Mb with imidazole. Titration experiments were carried out with imidazole on the lipid free HMP (O) and on HMP saturated with palmitoleic (□), cyclopropan-palmitoleic (Δ), and total *E. coli* lipid extracts (∇) in 0.1 M phosphate buffer at pH 7.0 and 20 °C. Control experiments have been also carried out on horse Mb in the presence (■) and in the absence (●) of TLE. Continuous lines represent fitting curves obtained by minimizing the experimental data to Schemes 1 and 2 (see Figure 1 and Table 2). The apparent equilibrium constant for imidazole binding to the protein saturated with palmitoleic, cyclopropan-palmitoleic, and total *E. coli* lipid extracts were 1.8 ± 0.5, 2.5 ± 0.7, and $3.6 \pm 0.2 \times 10^3$ M^{-1}, respectively.

around 6 s^{-1}. The origin of such a discrepancy has not been understood. Imidazole combination reaction of lipid free HMP (Figure 6A,B) also proceeded as an apparent single second-order process under a ligand concentration range that covered full saturation of the high affinity site and partial saturation of the low affinity site. The measured apparent combination rate was 4−5 faster than in lipid bound HMP yielding a value of 4×10^5 M^{-1} s^{-1}, as estimated from the pseudo-first-order plot of Figure 6B. The rate of imidazole release in the pseudo-first-order plot of Figure 6B seems to converge to about the same value as in the lipid bound protein. Obviously, it cannot be compared with the value(s) calculated from the equilibrium constants and the second-order rate constant. Thus, the whole set of imidazole binding time courses, measured on the lipid free protein, have also been fitted explicitly to Scheme 2 (Figure 1) by imposing the value of the equilibrium constants obtained from the fitting of the titration data. The values of the rate constants obtained from the global fitting procedure outlined in the Experimental Procedures are given in Table 2. Cyanide combination kinetics was also measured in both lipid free and lipid bound HMP (data not shown). Time courses were characterized by a second-order rate constant of 1.2×10^2 M^{-1} s^{-1} indicating that cyanide binding kinetics is insensitive to the presence of the bound lipid.

Heme−Iron Ligand Binding Properties of the Ferrous HMP. The ligand binding kinetic properties of the ferrous protein have been investigated by measuring the second-order binding rates of CO and the first-order kinetics of oxygen release on both the lipid free protein and the HMP saturated with different lipids or fatty acids. Lipid free HMP (data not shown) yielded biphasic second-order CO binding kinetics whose rates and amplitudes ($k_1 = 1.8 \times 10^7$ M^{-1} s^{-1} (68%) and $k_2 = 1.2 \times 10^6$ M^{-1} s^{-1} (32%)) were almost superimposable to those obtained by Gardner et al. (*5*). In contrast, experiments carried out on the protein saturated with TLE yielded perfectly monophasic CO ligand rebinding time courses after photolysis with a second-order rate of 5.1×10^6 M^{-1} s^{-1} (Figure 7). In Figure 7, the time course of CO rebinding after photolysis are shown in semilogarithmic plots. The absorbance decreases at 434 nm are the results of three linear records obtained in the nanosecond to millisecond time regime. In both lipid free and lipid saturated protein, no

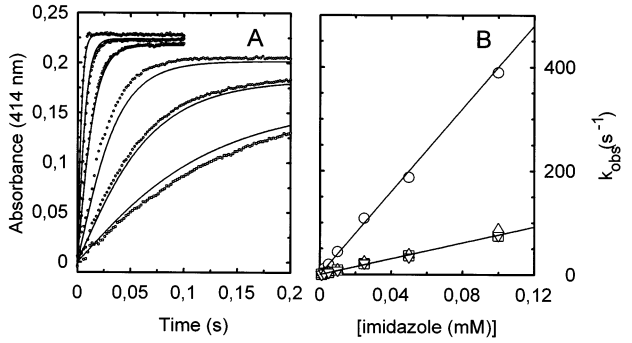

FIGURE 6: Imidazole combination kinetics to ferric *E. coli* flavohemoglobin. Panel A: imidazole combination time courses to ferric, lipid free HMP. Imidazole concentrations are reported in the abscissa of panel B. Continuous lines are the result of a global fitting procedure to Figure 1, Scheme 2 (see Experimental Procedures). The rate constants obtained are listed in Table 2. Panel B: Apparent pseudo-first-order rates of the time courses reported in panel A as a function of imidazole concentration. Continuous lines represent linear fits to the data and yield apparent second-order rate constants of $4.1 \pm 0.1 \times 10^5$ M^{-1} s^{-1} for imidazole binding to the lipid free protein and $8.5 \pm 0.2 \times 10^4$ M^{-1} s^{-1} for imidazole binding to HMP complexed with palmitoleic (○), ciclopropan palmitoleic (Δ), and TLE (total *E. coli* lipid extracts) (▽), respectively. Experiments were carried out in 0.1 M phosphate buffer, pH 7.0 and 20 °C. Protein concentration was 3−4 μM (after mixing).

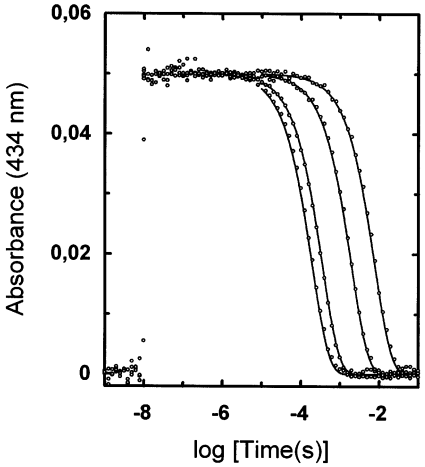

FIGURE 7: Kinetics of CO binding to ferrous *E. coli* flavohemoglobin. Time courses of CO recombination after photolysis of TLE treated HMP as a function of CO concentration. The experiment has been carried out in 0.1 M phosphate buffer at pH 7.0 containing 250 μM NADH and 1 mM EDTA at 20 °C (see Experimental Procedures). Continuous lines represent monoexponential fits to the experimental points that yield a second-order rate constant of $5.1 \pm 1.1 \times 10^6$ M^{-1} s^{-1}. The points in each data set (12 000 points merged from three different acquisitions in the nanosecond, microsecond, and millisecond time regime) have been logarithmically sampled.

geminate recombination processes were detected as demonstrated by the flatness of the nanosecond time recording. CO release kinetics were not measured due to the difficulty in obtaining unbiased time courses with the NO displacement method in the presence of a concomitant NO reduction (to N_2O) reaction. The kinetics of oxygen release, as monitored in oxygen pulse experiments (Figure 8), are likewise biphasic in lipid free HMP with first-order rates (k_{off}) of 2.2 s^{-1} (44%) and 0.11 s^{-1} (56%), respectively. In contrast, oxygen release from the TLE saturated protein are accounted for by a single-exponential decay ($k_{off} = 0.16$ s^{-1} at 20 °C). The behavior

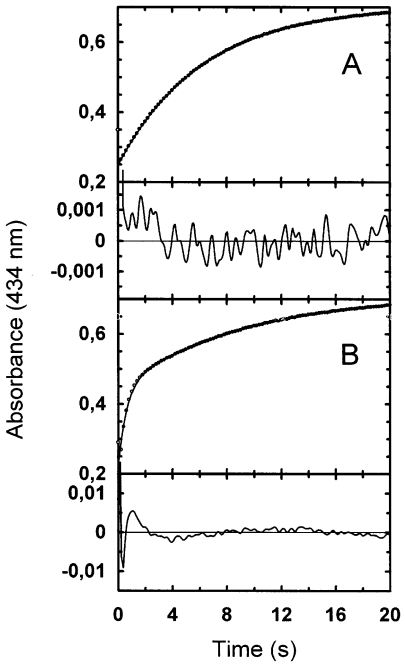

FIGURE 8: Kinetics of oxygen release in ferrous *E. coli* flavohemoglobin. Time courses of oxygen release from TLE treated and lipid free HMP (panels A and B, respectively) have been obtained in oxygen pulse experiments (see Experimental Procedures). Data in panel A have been fitted to a single-exponential decay with an apparent rate of 0.16 ± 0.01 s^{-1}. The kinetic record in panel B has been fitted to two exponentials characterized by apparent first-order rates of 2.2 ± 0.2 s^{-1} (44%) and 0.11 ± 0.03 s^{-1} (56%), respectively. The experiments have been carried out in 0.2 M phosphate buffer at pH 7.0 containing 25 mM sodium dithionite (after mixing) at 20 °C.

of O_2 release kinetics in HMP saturated with palmitoleic and cyclopropan-palmitoleic acid is an intermediate between the lipid free and TLE saturated HMP in that the amplitude of the fast phase is decreased but not abolished. Direct oxygen binding kinetics have not been reported. Laser photolysis experiments on the oxygenated derivative are in fact severely biased by the NADH driven oxygen consumption occurring during the experiments thus requiring more complex flow−flash measurements.

DISCUSSION

The present results demonstrate that HMP is capable of interacting with bacterial lipid membranes and is also able to recognize specifically UFA and/or CFA. These data challenge previous reports on *Vitreoscilla* Hb, *A. eutrophus* flavohemoglobin, and HMP itself that envisaged an unspecific interaction with membrane phospholipids (*8*, *9*). Most interestingly, binding of UFA or CFA to HMP gives rise to a clear spectroscopic change in the visible spectrum of the ferric heme. In fact, the absorption spectrum of the unliganded derivative corresponds to a typical pentacoordinated heme adduct in which the proximal histidine is the fifth ligand, as demonstrated by the peak at 645 nm and the broad Soret band, characterized by a low molar absorptivity and centered around 403 nm (*20*). In contrast, the spectrum of the UFA (or CFA) saturated species displays a sharp peak at 407 nm and a shallower one at 625 nm and is very similar to that of high spin adducts observed in many other hemoglobins and myoglobins in the presence of weak ligands

such as fluoride (*17*, *21*). Thus, the spectral profile of lipid bound HMP is diagnostic of the formation of a hexacoordinated species in which the sixth coordination position is occupied by a component of the fatty acid chain. This interpretation is consistent with the X-ray structural data by Ollesch et al. (*8*) on ferrous, lipid bound *A. eutrophus* flavohemoglobin. In fact, the electron density above the heme iron, taken together with the observed cis geometry of the *sn*-2 acyl chain within the heme pocket, has been identified as the cyclopropane ring of a *sn*-2 9,10-cyclopropan palmitoleic acid sitting on the top of the iron atom. Nevertheless, mass spectrometric investigation carried out in the same report revealed heterogeneity in the lipid composition thus suggesting that lipid binding was not specific (*8*). The present screening, carried out on a number of different (but homogeneous) lipids and fatty acids, brings about a different view. In fact, HMP is able to recognize UFA and CFA as free fatty acids, whereas no binding has been detected with saturated phosphatidil ethanolamine and phosphatidyl glycerol derivatives (the most abundant phospholipids within the *E. coli* membrane) nor with UFA or CFA methyl esthers. Furthermore, HMP does not bind saturated fatty acids nor simple linear or cyclic hydrocarbons containing cis double bonds.

Taken together, these observations indicate that two requisites are necessary for lipid recognition by HMP: (i) the presence of an anionic species, either carboxyl or phosphoryl, at one end of the acyl chain and (ii) the presence of a cis conformation of the acyl chain underlining unsaturation or cyclopropanation. On the basis of the observed spectral signal and on the structural data of Ollesh et al. (*8*), the physical nature of the double bond or cyclopropane ring recognition is most intriguing in that it seems to involve a weak but direct bonding interaction to the iron atom, at least in the ferric derivative. It may be envisaged that the iron−double bond interaction results from the superposition between the iron d_{z^2} orbital with the double bond π orbitals of appropriate symmetry. Such a lipid−protein interaction is unprecedented in all other hemoproteins investigated to date, including cyclooxigenases that have been shown to bind UFAs in a cavity located next to the heme pocket and not within the pocket itself (*22*). It is important, however, to point out that these spectral changes pertain uniquely to the ferric HMP derivative and that the UV−vis absorption spectra of the reduced derivatives (unliganded or CO bound) are not affected by the presence of UFA or CFA. Complete kinetic and thermodynamic parameters for fatty acid binding to ferric HMP have been obtained for linoleic acid only in the presence of ethanol (20%) as a cosolvent. The binding constant, estimated from ligand binding and release data (see Figures 2 and 3) is about 4×10^7 M^{-1} (or $k_d = 25$ nM), a figure that is similar to that of true type fatty acid binding proteins (*23*).

The observed specificity for UFA and CFA binding within the active site of HMP strongly suggested a possible enzymic activity toward these fatty acids. Mono/dioxygenation and/or hydroxylation reactions were screened on several UFAs and CFAs by means of ESI mass spectrometric analysis of fatty acid solutions incubated in the presence of NADH, oxygen, and variable amounts of protein (see Experimental Procedures and Table 1). Despite the high affinity for both oxygen and UFAs or CFAs and of the possibly favorable stereochemistry for oxygen addition to the acyl chain, no modifications of the fatty acid were detected under the experimental conditions used (i.e., pH 7.0, 20 °C, and NADH as a reductant, see Table 1). The absence of binding to pure DPPC liposomes (DPPC is not synthesized in bacteria) indicates that HMP can actually recognize the polar heads of naturally occurring phospholipids of *E. coli* membrane and does not interact with the hydrophobic core of the bilayer. The recent identification of an anion binding site (fully compatible with a phosphate binding site) in a protein loop above the heme pocket (*13*) allows one to hypothesize a recognition of the membrane through an interaction of the loop with the phosphate moiety of the phospolipid molecule. Thus, HMP most likely works at the interface between the cytosol and the bacterial inner membrane and is permanently saturated with a phospholipid esterified with either a UFA or a CFA molecule.

Heme−Iron Ligand Binding Properties of Ferric HMP. The broad, biphasic equilibrium titration profile for ligand binding to ferric, lipid free HMP and VHB (*13*, *18*) represents a puzzling thermodynamic behavior that had not been understood as yet. In a previous investigation, ligand binding to VHB was interpreted as an anticooperative behavior due to the apparently dimeric nature of the protein (*18*). Subsequently, the presence of a dimeric species in VHB has been challenged in an extensive ultracentrifugation investigation thus leaving the biphasic equilibrium ligand binding properties unexplained (*19*).

A complete reaction scheme (Figure 1) that takes into account the observed ligand binding profiles has been unraveled on the basis of a set of equilibrium and kinetic measurements carried out on both lipid bound and lipid free HMP (Figures 5 and 6). According to Scheme 1 (Figure 1), the lipid is weakly coordinated to the heme iron and is strongly bound to the non-heme site. Imidazole binding to the heme iron occurs upon displacement (not rate limiting, at least in the case of imidazole) of the weak iron−lipid bond and is entirely accounted for by a typical single site ligand binding process. The non-heme site must possess a very high affinity for the polar lipid head such that it cannot be displaced by heme iron ligands.

In the lipid free protein, the set of imidazole binding kinetics and equilibrium measurements suggested that the ligand might be able to occupy a protein site or cavity next to the heme that allows for rapid exchange with the heme iron. It is envisaged that the incoming ligand is coordinated by the heme iron ($k_1' > k_2'$) and then rapidly partitioned ($k_3' \approx k_3 > 1000$ s^{-1}) between the metal and the spectroscopically silent non-heme site (Figure 1, Scheme 2). This picture is in agreement with the presence of the two sites previously postulated for UFA recognition (i.e., the heme iron site that is capable of coordinating the acyl chain double bond (or cyclopropane ring) and a polar cavity that is necessary for harboring the polar head of the lipid). Thus, heme iron ligands might be hosted by the polar site in competition with the heme iron in the lipid free HMP.

The main question that arises from the proposed mechanism concerns the nature of the non-heme binding site and its unusual high affinity for the typical ferric heme iron ligands. Attempts to identify the non-heme site by direct X-ray diffraction measurements has failed in that ferric HMP crystals appear to grow only at pH 5.0 and thus under

unfavorable conditions for cyanide or imidazole binding (both ligands are protonated). Moreover, HMP crystals were also unstable upon increase in the pH values of the mother solution. Nevertheless, all X-ray diffraction maps thus obtained (including the deposited structure 1gvh, Brookhaven Protein Data Bank) do show electron density in a loop region above the heme pocket comprising residues Asp44−Arg54 (*13*). The electron density in the loop region has been assigned to a chloride ion although the geometry of the site shares some similarity to typical phosphate coordination regions. In particular, two Arg residues (Arg49 and Arg54) appear to provide a strong positive charge density that allows for coordination of anionic species. It may be envisaged that the loop region, which is endowed with high flexibility, is involved in the coordination of the fatty acid carboxyl and is also able to bind typical heme iron ligands. It is also worth recalling that conformational heterogeneity and hence high flexibility has been postulated to explain the lack of a definite diffraction pattern of the loop region above the heme pocket in ferric ligand free and ligand bound VHB (*12*, *18*).

Heme−Iron Ligand Binding Properties of Ferrous HMP. The effect of the bound lipid on the ferrous protein, although undetectable in the absorption spectra, manifests itself in both CO binding and oxygen release kinetics. It should be mentioned that the description of the CO and oxygen kinetic behavior is not complete in that no reliable data could be obtained on the oxygen binding process and on the CO release kinetics within the present experimental set up. Thus, the model described for imidazole binding in Scheme 2 (Figure 1) cannot be directly carried over the ferrous protein. Laser photolysis experiments on CO bound HMP revealed very fast and biphasic CO rebinding time courses in the lipid free protein, in agreement with the findings of Gardner et al. (*5*). In contrast, 10-fold slower and monophasic ligand rebinding kinetics are obtained in the TLE saturated HMP (see Figure 7). Oxygen release kinetics are also affected by the presence of a bound lipid. Lipid free protein is characterized by a strongly biphasic oxygen release kinetics whose rates and amplitudes are almost superimposable to those obatained on lipid free *Vitreoscilla* Hb (*18*). In contrast, a monoexponential ($0.16\ s^{-1}$) oxygen release process is observed in the lipid saturated protein (Figure 8).

These experimental observations offer further indications on the interplay between lipid binding and heme iron ligand binding in HMP. The absence of a heme spectroscopic signal in ferrous, lipid bound HMP is not surprising in that, as observed for most hemoglobins, weak ligands of the ferric heme (e.g., fluoride, nitrite, azide) are rapidly released upon iron reduction (*17*). Nevertheless, given the significant effect on the kinetic parameters of CO and oxygen binding/release, it must be envisaged that the lipid acyl chain is present in the heme pocket thus impairing CO binding and favoring oxygen release processes. Alternatively, the fatty acid might be bound to the non heme site and stabilize a single conformation that reacts slowly with CO and is capable of faster oxyen release (P* conformation). In turn, the lipid free protein must be endowed with a conformational equilibrium between two species to explain the heterogeneity observed in CO binding and oxygen release. These hypotheses (that are not mutually exclusive) may be reconciled with previous findings based on resonance Raman (*24*) and infrared spectroscopic (*14*) investigations (carried out on the lipid free protein) that envisaged the presence of two distinct conformers in the CO ligated species. The presence of two separate CO stretching frequencies had been attributed to the presence of an open and a closed conformer (*24*). In the closed conformer, it has been suggested that iron bound CO is stabilized by the TyrB10 phenol hydroxyl, whereas it is apparently free of constraint in the open conformation (*24*). Although the reaction Scheme 2 (Figure 1) cannot be easily carried over the ferrous protein, it is tempting to speculate that the closed conformation may correspond to the x−P∼ species, whereas the open conformation might be represented by the doubly x−P*∼(x) derivative. Interestingly, Scheme 2 (Figure 1) predicts that if the ligand binding rate (k_1') exceeds the rate of ligand exchange between the heme and the non-heme site (k_3'), biphasic ligand binding kinetics should be observed, as indeed observed for CO binding to the lipid free protein (5). X-ray studies on the ligand bound HMP are being actively pursued in the search of a structural confirmation of these hypotheses.

ACKNOWLEDGMENT

This paper is dedicated to the memory of Eraldo Antonini, unforgettable mentor, prematurely deceased 20 years ago on March 19th, 1983.

REFERENCES

1. Wittenberg, J. B., Bolognesi, M., Wittenberg, B. A., and Guertin, M. (2002) *J. Biol. Chem. 277*, 871−874.
2. Poole, R. K., Anjum, M. F., Membrillo-Hernandez, J., Kim, S. O., Hughes, M. N., and Stuart, V. (1996) *J. Bacteriol. 178*, 5487−5492.
3. Gardner, P. R., Gardner, A. M., Martin, L. A., and Salzman, A. L. (1998) *Proc. Natl. Acad. Sci. U.S.A. 95*, 10378−10383.
4. Hausladen, A., Gow, A. J., and Stamler, J. S. (1999) *Proc. Natl. Acad. Sci. U.S.A.* 95, 14100−14105.
5. Gardner, A. M., Martin, L. A., Gardner, P. R., Dou, Y., and Olson, J. S. (2000) *J. Biol. Chem. 275*, 12581−12589.
6. Membrillo-Hernandez, J., Ioannidis, N., and Poole, R. K. (1996) *FEBS Lett. 382*, 141−144.
7. Hausladen, A., Gow, A., and Stamler, J. S. (2001) *Proc. Natl. Acad. Sci. U.S.A. 98*, 10108−10112.
8. Ollesch, G., Kaunzinger, A., Juchelka, D., Schubert-Zsilavec, M., and Ermler, U. (1999) *Eur. J. Biochem. 262*, 396−405.
9. Ramandeep, Hwang, K. W., Raje, M., Kim, K. J., Stark, B. C., Dikshit, K. L., and Webster, D. A. (2001) *J. Biol. Chem. 276*, 24781−24789.
10. Pathania, R., Navani, N. K., Rajamohan, G., and Dikshit, K. L. (2002) *J. Biol. Chem. 277*, 15293−15302.
11. Ermler, U., Siddiqui, R. A., Cramm, R., and Friedrich, B. (1995) *EMBO J. 14*, 6067−6077.
12. Tarricone, C., Galizzi, A., Coda, A., Ascenzi, P., and Bolognesi, M. (1997) *Structure 14*, 497−507.
13. Ilari, A., Bonamore, A., Farina, A., Johnson, K. A., and Boffi, A. (2002) *J. Biol. Chem. 277*, 23725−23732.
14. Bonamore, A., Chiancone, E., and Boffi, A. (2001) *Biochim. Biophys. Acta 1549*, 174−178.
15. Bligh, E. G., and Dyer, W. J. (1959) *Can. J. Biochem. Physiol. 37*, 911−917.
16. Chiancone, E., Anderson, N. M., Antonini, E., Bonaventura, J., Bonaventura, C., Brunori, M., and Spagnuolo, C. (1974) *249*, 5689−5694.
17. Antonini, E., and Brunori, M. (1971) in *Hemoglobin and Myoglobin in Their Reactions with Ligands* (Neuberger, A., and Tatum, E. L., Eds.) pp 235−260, North-Holland Publishing Co., Amsterdam.
18. Bolognesi, M., Boffi, A., Coletta, M., Mozzarelli, A., Pesce, A., Tarricone, C., and Ascenzi, P. (1999) *J. Mol. Biol. 291*, 637−650.

19. Giangiacomo, L., Mattu, M., Arcovito, A., Bellenchi, G., Bolognesi, M., Ascenzi, P., and Boffi, A. (2001) *Biochemistry 40*, 9311−9316.
20. Boffi, A., Das, T. K., della Longa, S., Spagnuolo, C., and Rousseau, D. L. (1999) *Biophys. J. 77*, 1143−1149.
21. Eaton, W. A., and Hofrichter, J. (1981) *Methods Enzymol. 76*, 175−261.
22. Marnett, L. J., Rowlinson, S. W., Goodwin, D. C., Kalgutkar, A. S., and Lanzo, C. A. (1999) *J. Biol. Chem. 274*, 22903−22906.
23. Ganesaratnam, K. B., Scnutgen, F., Scapin, G., Borchers, T., Xhong, N., Lim, K., Godbut, R., Spener, F., and Sacchettini, J. C. (2000) *J. Biol. Chem. 275*, 27045−27054.
24. Mukai, M., Mills, C. E., Poole, R. K., and Yeh, S. R. (2001) *J. Biol. Chem. 276*, 7272−7277.

BI0206311